MedChemComm

RESEARCH ARTICLE

View Article Online
View Journal | View Issue

Cite this: *Med. Chem. Commun.*, 2018, **9**, 1698

Structural optimization and antibacterial evaluation of rhodomyrtosone B analogues against MRSA strains†

Liyun Zhao,‡[ac] Hongxin Liu,‡[ab] Luqiong Huo,[ac] Miaomiao Wang,[ac] Bao Yang,[a] Weimin Zhang,[b] Zhifang Xu,[a] Haibo Tan*[a] and Sheng-Xiang Qiu *[a]

Received 17th May 2018,
Accepted 9th August 2018

DOI: 10.1039/c8md00257f

rsc.li/medchemcomm

Methicillin-resistant *Staphylococcus aureus* (MRSA) infections are well-known as a significant global health challenge. In this study, twenty-two congeners of the natural antibiotic rhodomyrtosone B (RDSB) were synthesized with the aim of specifically enhancing the structural diversity through modifying the pendant acyl moiety. The structure–activity relationship study against various MRSA strains revealed that a suitable hydrophobic acyl tail in the phloroglucinol scaffold is a prerequisite for antibacterial activity. Notably, RDSB analogue **11k** was identified as a promising lead compound with significant *in vitro* and *in vivo* antibacterial activities against a panel of hospital mortality-relevant MRSA strains. Moreover, compound **11k** possessed other potent advantages, including breadth of the antibacterial spectrum, rapidity of bactericidal action, and excellent membrane selectivity. The mode of action study of compound **11k** at the biophysical and morphology levels disclosed that **11k** exerted its MRSA bactericidal action by membrane superpolarization resulting in cell lysis and membrane disruption. Collectively, the presented results indicate that the novel modified RDSB analogue **11k** warrants further exploration as a promising candidate for the treatment of MRSA infections.

1. Introduction

Infectious diseases are one of the major causes responsible for human death worldwide, particularly in developing countries.[1,2] Methicillin-resistant *Staphylococcus aureus* (MRSA) is well-known as a pathogenic bacterium giving rise to terrible infections, associated with high rates of morbidity and mortality.[3,4] MRSA infection is considered as one of the most intractable diseases because of its emerging resistance, exhibiting resistance to almost every commercially available antibiotic, including β-lactam,[5] macrolide,[6] fluoroquinolone,[7] aminoglycoside,[8] tetracycline,[9] and lincosamide antibiotics,[9] with numerous resistance mechanisms.[10] As a result, the therapeutic options for the treatment and control of MRSA infections are very limited,[11] and it has now been declared a public-health imperative.[3,10,12] Therefore, the discovery of potential new agents to control multidrug-resistant pathogens is crucial to the maintenance of public health in the near future.[13]

In our continuous campaign to find novel antibiotics from traditional Chinese medicinal plants or through synthesis to counter the threat of MRSA bacteria,[14–17] we have recently reported two natural acylphloroglucinols (Scheme 1), rhodomyrtone and rhodomyrtosone B (RDSB),[15] which were reputed to exhibit significant antibacterial activity against Gram-positive pathogens, even including MRSA, with novel mechanisms.[18–20] However, the paucity of rhodomyrtone's natural supply and its inconvenient total synthesis make the prospects for structural optimization of rhodomyrtone seem distinctly challenging and rather bleak.[21] Although RDSB did not attract any attention or become widely accepted by medicinal scientists, even though the details of its chemical synthesis have been well established, its comparable antibacterial activity with that of rhodomyrtone and much more accessible synthesis make it also an appealing lead compound for new antibacterial drug discovery. In this regard, an effort towards the design and synthesis of novel RDSB analogues, which would facilitate convergent assembly in conjunction with considerable antibacterial activity, seemed to be worthy of pursuit.

[a] *Key Laboratory of Plant Resources Conservation and Sustainable Utilization, South China Botanical Garden, Chinese Academy of Sciences, Guangzhou, 510650, People's Republic of China. E-mail: tanhaibo@scbg.ac.cn, sxqiu@scbg.ac.cn*
[b] *State Key Laboratory of Applied Microbiology Southern China, Guangdong Provincial Key Laboratory of Microbial Culture Collection and Application, Guangdong Open Laboratory of Applied Microbiology, Guangdong Institute of Microbiology, Guangzhou 510070, People's Republic of China*
[c] *University of Chinese Academy of Sciences, Beijing 100049, People's Republic of China*

† Electronic supplementary information (ESI) available. See DOI: 10.1039/c8md00257f

‡ These authors contributed equally to this work.

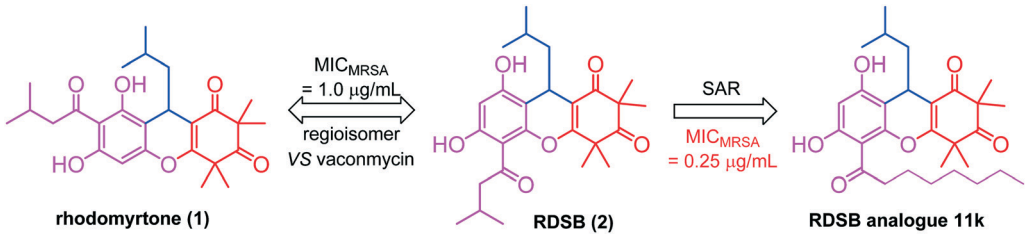

Scheme 1 The structure of rhodomyrtone, RDSB, and their analogue **11k**.

Herein, we describe our efforts, accompanied by a full exploration of the details of the synthesis of the RDSB analogues, their antibacterial evaluations, lead structural optimization through extensive structure–activity relationship (SAR) investigations, and their antibacterial mechanism.

2. Results and discussion

2.1. Chemistry

The implementation of the chemical synthesis of RDSB analogues **11** was commenced with the preparation of syncarpic acid (7) by the previously established protocol with slight modification, as shown in Scheme 2.[21,22] Following this, the syncarpic acid (7) could be readily accessed through a standard sequence of aluminum trichloride-catalyzed Friedel–Crafts acylation, selective C-tetramethylation, and retro-Claisen condensation. On treating the syncarpic acid (7) with isovaleraldehyde, the proline-promoted Knoevenagel condensation reaction would take place smoothly to provide the critical intermediate **9** within almost quantitative yield (95% yield).[22] The crucial coupling of intermediate **9** and the relative acetylphloroglucinols **5** was initiated at room temperature in THF under strong basic conditions. Satisfyingly, the reaction conditions seemed to be compatible with a series of acetylphloroglucinol substrates, tending to provide every desired acyclic product **10** in excellent yields ranging from 88% to 96%. Further intramolecular cyclization, enabled by treating acyclic acetylphloroglucinols **10** with PTSA (1.0 equiv.) in refluxing toluene, was totally completed in 1 hour and delivered all of the corresponding RDSB analogues **11** in more than 80% yield.[21] The structures of all of the new RDSB analogues **11** were fully characterized and confirmed by HRMS, ^{1}H NMR, and ^{13}C NMR spectra.

2.2. Biological evaluation

2.2.1. Antibacterial activity of RDSB analogues 11. The minimum inhibitory concentration (MIC) for RDSB analogues **11** against MRSA cells (JCSC 4788) was evaluated by means of the micro dilution susceptibility test, performed in Mueller–Hinton broth (MHB) following CLSI guidelines and using vancomycin as the positive control. The highest MIC for the tested acylphloroglucinol analogues **11** was 256 μg mL^{-1}, indicating their potent antibacterial activities. Moreover, all of the synthesized compounds **11** were also tested for their antibacterial activity against standard *Staphylococcus aureus* (ATCC 6538). The results are listed in Table 1, and the data were obtained with vancomycin as the standard. Results

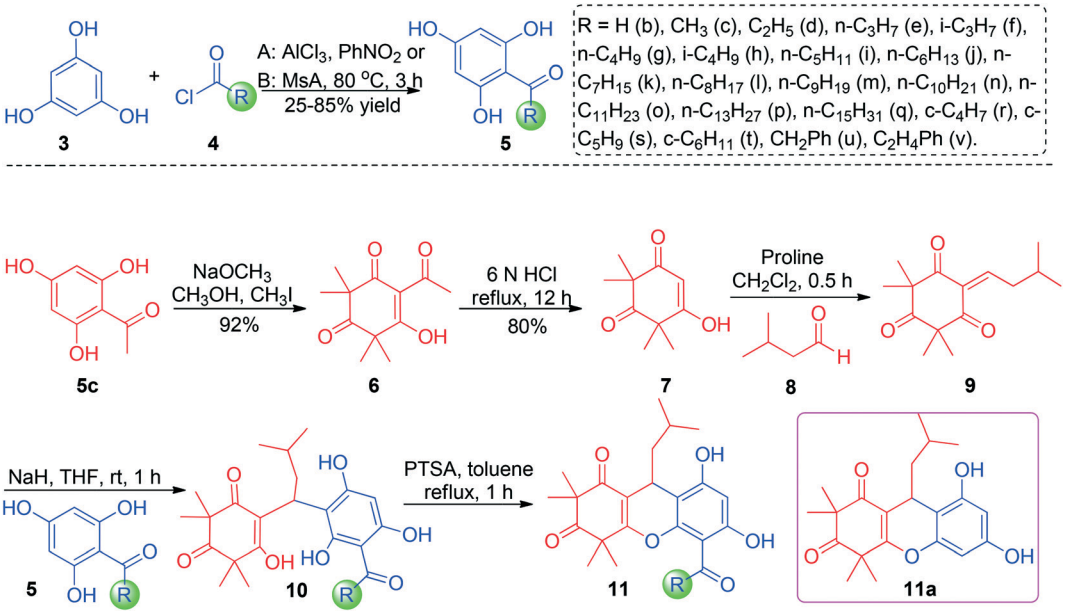

Scheme 2 The synthesis of RDSB analogues **11**.

Table 1 *In vitro* antibacterial evaluation (MIC) of RDSB analogues **11a–11v** against MRSA (JCSC 4788) and standard SA (ATCC 6538)

Comp.	R	MIC_{MRSA} μg mL^{-1}	MIC_{SA} μg mL^{-1}	Comp.	R	MIC_{MRSA} μg mL^{-1}	MIC_{SA} μg mL^{-1}
11a	—	256	>256	**11l**	*n*-C_8H_{17}	0.5	0.25
11b	H	128	128	**11m**	*n*-C_9H_{19}	0.50	0.50
11c	CH_3	4.0	4.0	**11n**	*n*-$C_{10}H_{21}$	1.0	1.0
11d	C_2H_5	2.0	2.0	**11o**	*n*-$C_{11}H_{23}$	8.0	8.0
11e	*n*-C_3H_7	2.0	2.0	**11p**	*n*-$C_{13}H_{27}$	256	128
11f	i-C_3H_7	4.0	4.0	**11q**	*n*-$C_{15}H_{31}$	>256	>256
11g	*n*-C_4H_9	1.0	0.5	**11r**	*c*-C_4H_7	8.0	4.0
11h	i-C_4H_9	1.0	0.5	**11s**	*c*-C_5H_9	4.0	4.0
11i	*n*-C_5H_{11}	0.5	0.5	**11t**	*c*-C_6H_{11}	4.0	2.0
11j	*n*-C_6H_{13}	0.5	0.25	**11u**	CH_2Ph	4.0	4.0
11k	*n*-C_7H_{15}	0.25	0.25	**11v**	C_2H_4Ph	2.0	2.0
1	—	1.0	1.0	**Van.**	—	1.0	0.5

from anti-MRSA screening demonstrated a clear structure–activity relationship, wherein the lipophilic ability of the acyl group tails had a significant influence on the potency of bacterial growth inhibition.

2.2.2. Structure activity relationship study of RDSB analogues 11. Ketone motifs are usually considered to be one of the most ubiquitous and intriguing functional groups in the repertoire of medicinal chemistry, forming the basic active moieties for various biologically meaningful natural products and pharmaceuticals. Therefore, an initial effort was conducted to unravel the mystery of the role of the ketone moiety in the RDSB analogues, which might subsequently serve as an informative vehicle for the rational structure design of lead compounds. As expected, the compound **11b**, whose lipophilic ketone tail was replaced by an aldehyde group, showed dramatically weak antibacterial activity even at 128 μg mL^{-1}, strongly indicating that the hydrophobic acyl tail and the ketone moiety in the phloroglucinol core are vital elements in maintaining the biological properties (Table 1). In addition, compound **11a** without the acetyl tail was devoid of any noticeable activity against these same strains at a concentration even up to 256 μg mL^{-1}, further consolidating this conclusion.

Biophysical processes play a significant role in the antimicrobial activity, especially for amphiphilic molecules.[16,23,24] Thus, it could be readily anticipated that suitable tuning of the amphiphilic property of the target molecule would result in a critical influence on its biological activities. With this scenario in mind, the effect on bactericidal activity of hydrophobic acetyl tails with different lengths was evaluated. The anti-MRSA activity was found to linearly correlate with the enhancing lipophilicities of the acetyl tail in **11c–11k**. Moreover, when more lipophilic acetyl tails were induced in the RDSB analogues **11g–11n**, neither the length nor the lipophilicity of the acetyl tails seemed to have a significant influence on the anti-MRSA activity, giving rise to potent anti-MRSA activity with the MIC values ranging from 0.25–1.0 μg mL^{-1}, similar to that of vancomycin (MIC = 1.0 μg mL^{-1}). Notably, if the length of the acetyl tails was more than 11 carbons, the more lipophilic properties had a detrimental effect on the antibacterial activity. In particular, **11q** showed no bacterial inhibition even at 128 μg mL^{-1}. Moreover, a cyclic ring in the hydrophobic acetyl tail seemed not to significantly affect the antibacterial activity, as clarified with **11r–11v**.

Although the lipophilicity seemed to be the principal factor influencing the antibacterial activity, both the hydrophobicity and length of the acyl tail significantly modulate their antibacterial potency, which was not linearly correlated with their lipophilicity. These results were attributed to the penetrability of the RDSB analogues to diffuse into the MRSA membrane to reach their antibacterial site. However, it was clear that the lipophilicity might be the most important physicochemical property for determining the antibacterial activity of the RDSB analogues. For the more active RDSB analogues, suitable lipophilicity is a prerequisite and the optimal length for the acetyl tail was found to be between 4 and 9 carbons. As shown in the context of the structure–activity relationship investigation, the most active RDSB analogue was found to be **11k** (molecular weight = 470.27), which showed profound anti-MRSA activity with an MIC value as low as 0.25 μg mL^{-1} towards MRSA cells (JCSC 4788). Its activity was similar to that for the clinical drug vancomycin (MIC = 1.0 μg mL^{-1}, molecular weight = 1485.71), an agent of last resort for the treatment of severe MRSA infections; thus, finding alternative therapeutic options is critical to address the burden of vancomycin.

2.2.3. The antibacterial spectrum evaluation of RDSB analogue 11k. Motivated by the success of **11k** with promising anti-MRSA activity, an effort to assess its antibacterial spectrum was further conducted against a broad array of clinically relevant multidrug-resistant MRSA isolates and common bacteria. As expected, **11k** successfully maintained its potent antibacterial activity with MICs identical to or 0.5 to 2-fold higher than that reported for MRSA JCSC 4788 against all of the tested MRSA isolates ((JCSC 2172), (JCSC 3063), (JCSC 4469), (JCSC 4744), (NCTC 10442), (N 315), and (85/2082)), and even against VRE (No. 151458137) at MIC = 2.0 μg mL^{-1} (Table 2), which strongly suggests that the RDSB analogue **11k** can satisfactorily overcome its cross-resistance with commonly used clinical antibiotics (Table 2). Moreover, **11k** also exhibited potent activity against all other tested Gram-positive bacterial strains such as *S. aureus* (ATCC 6538), *S.*

Table 2 Antibacterial spectrum of **11k** against various bacteria

Bacteria	G^+/G^-	MIC (μg mL^{-1})		
		RDSB	**11k**	Vancomycin
S. aureus (ATCC 29213)	G^+	1.0	0.50	1.0
S. aureus (ATCC 6538)	G^+	1.0	0.25	1.0
S. aureus (CMCC 26003)	G^+	0.50	0.25	0.50
MRSA (JCSC 4788)	G^+	1.0	0.50	1.0
MRSA (JCSC 2172)	G^+	0.50	0.25	1.0
MRSA (JCSC 3063)	G^+	0.50	0.25	1.0
MRSA (JCSC 4469)	G^+	0.50	0.25	0.50
MRSA (JCSC 4744)	G^+	0.50	0.125	1.0
MRSA (NCTC 10442)	G^+	1.0	0.50	1.0
MRSA (N315)	G^+	1.0	0.25	1.0
MRSA (85/2082)	G^+	1.0	0.25	1.0
B. cereus (ATCC 10876)	G^+	0.50	0.50	0.50
P. acnes (ATCC 6919)	G^+	0.50	0.25	0.50
E. faecalis (ATCC 29212)	G^+	1.0	0.25	0.50
S. epidermidis (ATCC 12228)	G^+	1.0	0.25	0.50
VRE (No. 151458137)	G^+	2.0	2.0	>32
B. polymyxa (GIM 1.467)	G^+	>32	>32	>32
B. polymyxa (ATCC 842)	G^+	>32	>32	>32
E. coli (ATCC 8739)	G^-	>32	>32	>32
S. typhi (CMCC 44102)	G^-	>32	>32	>32
S. dysenteriae (CMCC 51252)	G^-	>32	>32	>32
C. albicans (ATCC 10231)	Fungi	>32	>32	>32

aureus (CMCC 26003), *B. cereus* (ATCC 10876), *P. acnes* (ATCC 6919), *E. faecalis* (ATCC 29212), and *S. epidermidis* (ATCC 12228) with MIC values ranging from 0.125 to 0.5 μg mL^{-1}, demonstrating superior potency to that of the control drug vancomycin (Table 2) and a widely diverse antibacterial spectrum. On the other hand, when the Gram-positive bacteria *B. polymyxa* (GIM 1.467) and *B. polymyxa* (ATCC 842), the Gram-negative bacteria *E. coli* (ATCC 8739), *S. typhi* (CMCC 44102) and *S. dysenteriae* (CMCC 51252), and fungus *C. albicans* (ATCC 10231) were tested, **11k** showed no noticeable biological effects (MIC >32 μg mL^{-1}); this collectively indicated that **11k** is a promising selective antibacterial agent. *B. polymyxa* represents an exception to the general rule that Gram-positive bacteria have a low content of PE compared with Gram-negative bacteria,[25] and the difference in the lipid composition of the bacterial membranes between specific and non-specific bacteria will be helpful for finding molecular targets of **11k** in future work.

2.2.4. Toxicity analysis of potent RDSB analogue 11k against mammalian cells. To further evaluate the selectivity of antibacterial *versus* antiproliferative activities, the most active RDSB analogue **11k** was next subjected to a preliminary cytotoxicity profiling. Hence, compound **11k** was evaluated against the RAW 264.7 cell line and the cancer cell lines MCF-7 and SF-268 to determine the potential toxic effect *in vitro* after 24 h of exposure. As depicted in Table 3, the IC_{50} of **11k** against RAW cells was 5.6 ± 0.42 μg mL^{-1}, which was more than 20-fold higher than the MIC value (0.25 μg mL^{-1}) obtained against MRSA. Compound **11k** exhibited insignificant toxicity to RAW 264.7 cells when 0.25 μg mL^{-1} **11k** was used to kill MRSA cells. The IC_{50} of **11k** against cancer cells MCF-7 and SF-268 was 9.98 ± 1.08 and 10.15 ± 0.98 μg mL^{-1}, respectively. These positive results indicated that **11k** could emerge as a promising candidate and merits further consideration for the development of novel anti-MRSA therapeutic agents.

Table 3 The anti-MRSA selectivity *versus* antiproliferative (IC_{50}) activity against RAW 264.7, MCF-7 and SF-268 cells

	RAW 264.7	MCF-7	SF-268
IC_{50} (μg mL^{-1})	5.6 ± 0.42	9.98 ± 1.08	10.15 ± 0.98
Selectivity ratio[a]	22.4	39.9	40.6

[a] Selectivity ratio = IC_{50}/MIC against MRSA (JCSC 4788).

2.2.5. Time-kill assay of RDSB analogue 11k against MRSA (JCSC 4788) cells. Glycopeptides such as vancomycin and oxazolidinones such as linezolid are well-known as two cornerstone clinical antimicrobials responsive for the treatment of systemic MRSA infections, but both of them have unavoidable drawbacks influencing their clinical efficiency, namely linezolid being a bacteriostatic agent and slow bactericidal action for vancomycin,[26] which usually result in intractable problems for patient rehabilitation or clinical failure in many cases.[27,28] In order to confirm the bactericidal activity of the new RDSB analogues, the most promising compound **11k** was further evaluated against MRSA (JCSC 4788) cells in comparison with the known bactericidal agent vancomycin using a standard time-kill kinetics assay ranging from 0.5 to 4.0× MIC. As presented in Fig. 1, time-kill kinetic experiments dosing with 0.5 and 1.0× MIC suppressed more than 90% of bacterial growth within 8 h, revealing a considerable bactericidal effect. When higher concentrations of **11k** (2.0 and 4.0× MIC) were tested, the time-kill kinetic experiments unambiguously disclosed that **11k** exhibited a very rapid *in vitro* bactericidal activity (killing >90% MRSA cells within 2.0 and 0.5 h respectively) and a complete bactericidal effect with a sharp reduction in CFU of 99.9% after 2 and 4 h of exposure, respectively. Meanwhile, vancomycin only achieved a 99.9% reduction at the same concentration in more than 8 h. In this respect, RDSB analogue **11k** exhibited a distinctly superior advantage over vancomycin because of its rapid time-kill effect. This experimental evidence indicated that the RDSB analogue **11k** mainly exerted bactericidal activity at a dose of more than 2-fold the MIC with rapid efficiency.

2.3. Bactericidal mechanism study

2.3.1. The effect on the MRSA membrane probed by DiSC3(5) and SYTOX Green assay. In order to understand the anti-bacterial mode of action for RDSB analogue **11k** at the morphological level and shed light on the mechanism underlying the antimicrobial activity against the clinical MRSA isolate (JCSC 4788), a mechanistic investigation using fluorescent probes was initiated combining the well-known fluorescence agents DiSC3(5) and SYTOX Green through fluorescence imaging technology.[16,29] As shown in Fig. 2A, after treating the MRSA (JCSC 4788) cells with serial

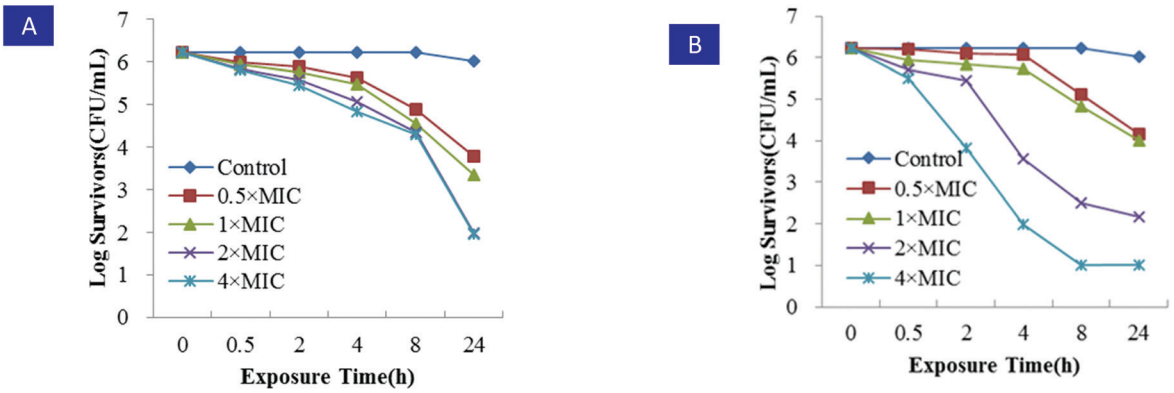

Fig. 1 Time-kill kinetics of MRSA (JCSC 4788). A) Vancomycin, MIC value (μg mL^{-1}): vancomycin = 1.0; B) **11k**, MIC value (μg mL^{-1}): **11k** = 0.25.

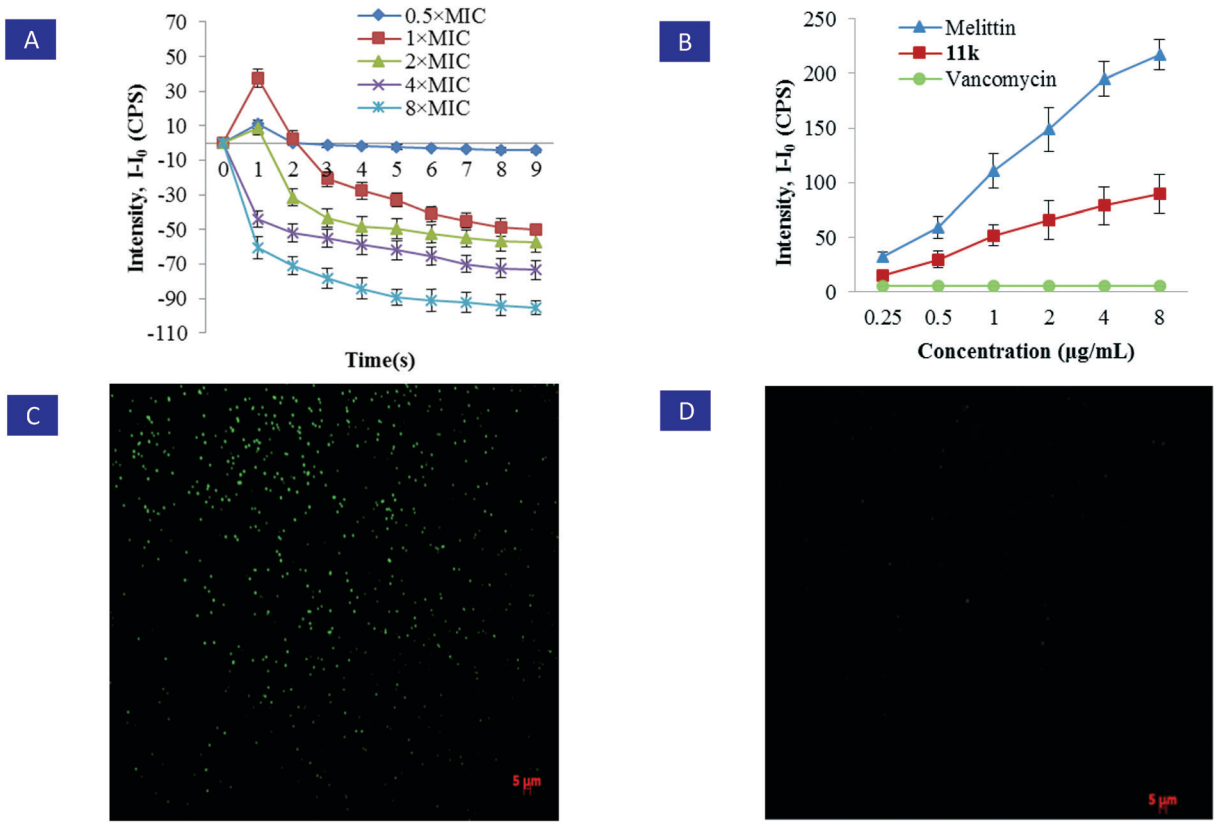

Fig. 2 Hyperpolarization of the bacterial cytoplasmic membrane. A) The fluorescence of the dye DiSC3(5) within a MRSA (JCSC 4788) bacterial suspension was monitored with a spectrophotometer. B) The use of SYTOX Green demonstrated that treatment with over 1× MIC RDSB **11k** for 3 h induced membrane disruption of MRSA (JCSC 4788). In contrast, no increase in fluorescence was observed when vancomycin was added. Melittin was used as a positive control. Error bars represent the standard deviation, n = 3. C) Compound **11k** compromised the inner membrane of MRSA and caused significant increases in fluorescence emission due to SYTOX Green binding to nucleic acids. D) In contrast, no significant fluorescence emission was observed, when MRSA was treated with vancomycin.

concentrations of **11k** (0.5× MIC, 1× MIC, 2× MIC, 4× MIC, 8× MIC), the depolarization of the bacterial membrane potential was intermediately induced within 1 min at 0.5–2× MIC, because an obvious increase of fluorescence was observed. However, a significant decrease in the fluorescence intensity was observed after more than 2 min at 1–2× MIC and in the whole process at 4–8× MIC, suggesting that the favorable bactericidal action of **11k** might be attributed to a decrease of the membrane potential due to its hyperpolarization.

Moreover, the SYTOX Green assay indicated that RDSB analogue **11k** showed an excellent ability to disrupt and permeabilize the bacterial inner membrane, since an obvious increase in fluorescence intensity was detected when the MRSA suspension was treated even with 1× MIC for only 3 h. In comparison, the positive control melittin also caused an unambiguous increase in fluorescence in the whole concentration range from 0.25 to 8 μg mL^{-1} after 3 h, whereas the negative control vancomycin failed (Fig. 2B). Moreover, this

aforementioned conclusion was further confirmed by the observation of the staining of **11k**-treated bacteria using fluorescence microscopy. As a result, a large number of stained bacteria were observed in a culture incubated with **11k**, clearly clarifying that it compromised the living bacterial cytoplasmic membrane. Hence, these informative results collectively pointed to a rational conclusion that the RDSB analogue **11k** resulted in Gram-positive bacterial death by disrupting their membranes.

2.3.2. The visualization of cells by SEM. The morphological changes of the MRSA (JCSC 4788) cells after treatment with RDSB analogue **11k** were then examined using scanning electron microscopy (SEM), and the result was in good agreement with that of the fluorescence probes, wherein RDSB analogue **11k** successfully disrupted the cytoplasmic membrane structure of MRSA (JCSC 4788) cells following treatment with 4× MIC of **11k** for 3 h. As shown in Fig. 3, the bacterial membrane exhibited extensive damage, and almost all of the tested MRSA cells were obviously distorted with intracellular components released. However, the morphology of the untreated cells remained intact with smooth spheres. The findings of rapid structural effects and apparent membrane changes also agreed well with the results of the time-kill assays. Based on the results of the membrane hyperpolarization and membrane disruption assays, in conjunction with the time-killing study (killing >99.9% after 4 h), it can be concluded that RDSB analogue **11k** acts rapidly as a bactericidal antibiotic to induce cell lysis by causing membrane hyperpolarization and disruption.

2.4. Multistep drug-resistance assay

The emerging drug-resistance has been considered as one of the most intractable problems for the treatment of infectious diseases; however, a membrane-targeting agent would be very unlikely to lead to resistance, since the membrane-targeted mechanism would require the bacteria to change their entire membrane chemistry, which would almost certainly lead to the cells being unviable. With this scenario, the membrane-targeting action of RDSB analogue **11k** is expected to play an important role in minimizing the development of drug-resistance because of its rapid bactericidal action through membrane disruption. As expected, when a multipassage resistance study was conducted with serial passaging in the presence of sub-MIC levels of antimicrobial drug **11k**, no detectable resistance was observed even after 20 serial passages (Fig. 4). However, in the equivalent case of ofloxacin, the MIC value began to increase after 5 passages and had increased 16 times after 20 passages. Therefore, this result strongly demonstrated that RDSB analogue **11k** resulted in significant suppression of MRSA drug-resistance activity and was suitable for further clinical applications.

2.5. The *in vivo* efficacy of RDSB analogue 11k in MRSA-infected mice

Motivated by its potent bactericidal activity and attractive selectivity profiles, RDSB analogue **11k** was then evaluated in a mouse skin infection model against MRSA (JCSC 4788) to assess its *in vivo* antibacterial efficacy. Compared to untreated controls, a single dose of RDSB analogue **11k** or vancomycin was observed to significantly prevent skin ulcer formation (Fig. 5A).

In addition, RDSB analogue **11k** treated animals showed significantly lower incidence of infection-induced morbidity, as evaluated by weight loss (Fig. 5B) and wound size (Fig. 5C). These initial investigations clearly proved that RDSB analogue **11k** had significant therapeutic efficacy to suppress the virulence of MRSA *in vivo*.

3. Conclusion

In summary, we report the synthesis and anti-MRSA activity of a pool of twenty-two synthetic natural product-based RDSB analogues with enhanced structural diversity, synthesized through a new strategy of modifying the pendant acyl moiety.

The SAR study against the MRSA (JCSC 4788) strain clearly suggested that the presence of an optical hydrophobic acyl tail in the phloroglucinol scaffold was a prerequisite for the anti-bacterial activity of the RDSB analogues. The reasons underlying the aforementioned observation might be attributed

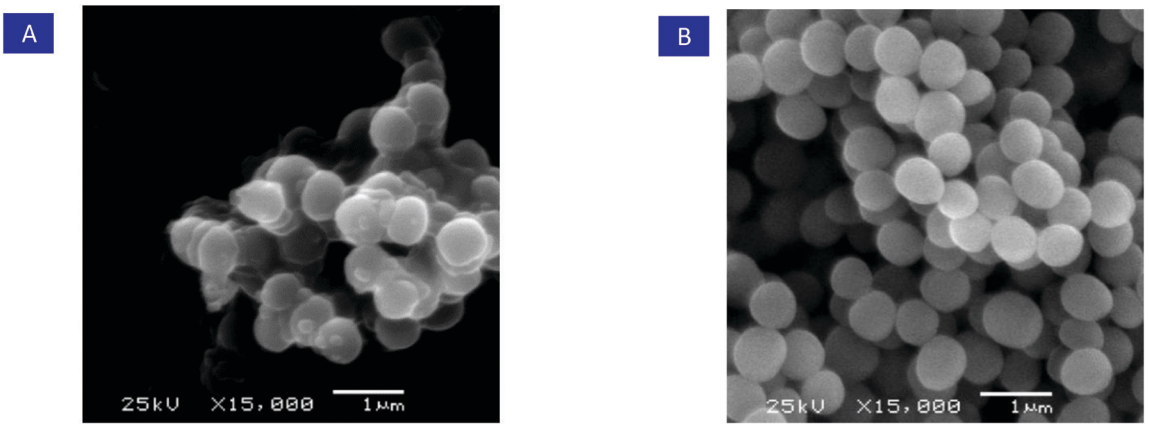

Fig. 3 A) SEM of MRSA treated with **11k**. B) SEM of untreated MRSA.

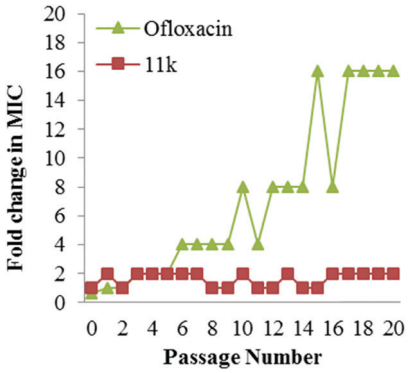

Fig. 4 Resistance acquisition during serial passaging in the presence of sub-MIC levels of antimicrobial drugs. Ofloxacin was used as a positive control.

to these substituents increasing the ability of the compounds to penetrate the bacterial cell wall and distort the MRSA cell membrane. Among them, RDSB analogue **11k** was identified as a very promising lead compound with significant antibacterial activity against a wide panel of MRSA strains with similar activity to the reference antibiotic vancomycin. Most importantly, compound **11k** possessed profound *in vivo* antibacterial anti-MRSA activity and many other admirable features, including breadth of the antibacterial spectrum, rapidity of bactericidal action, and excellent membrane selectivity. Moreover, the investigation of its biophysical and morphological effects revealed that **11k** exerted a bactericidal action on MRSA strains by membrane hyperpolarization to induce membrane disruption, which represents a very favorable bactericidal mechanism, rendering it a very promising candidate for further extensive medicinal chemistry investigations with an aim towards antibiotic drug discovery with novel chemical scaffolds and mechanisms of action.

4. Experimental section

4.1. Materials and experimental apparatus

All of the reactions were carried out under nitrogen atmosphere with dry solvents under anhydrous conditions, unless otherwise noted. Reagents were purchased at high commercial quality and used without further purification. Thin-layer chromatography (TLC) was conducted with 0.25 mm Tsingdao silica gel plates (60 F-254) and visualized by exposure to UV light (254 nm) or staining with potassium permanganate. Silica gel (ZCX-II, 200–300 mesh) used for flash

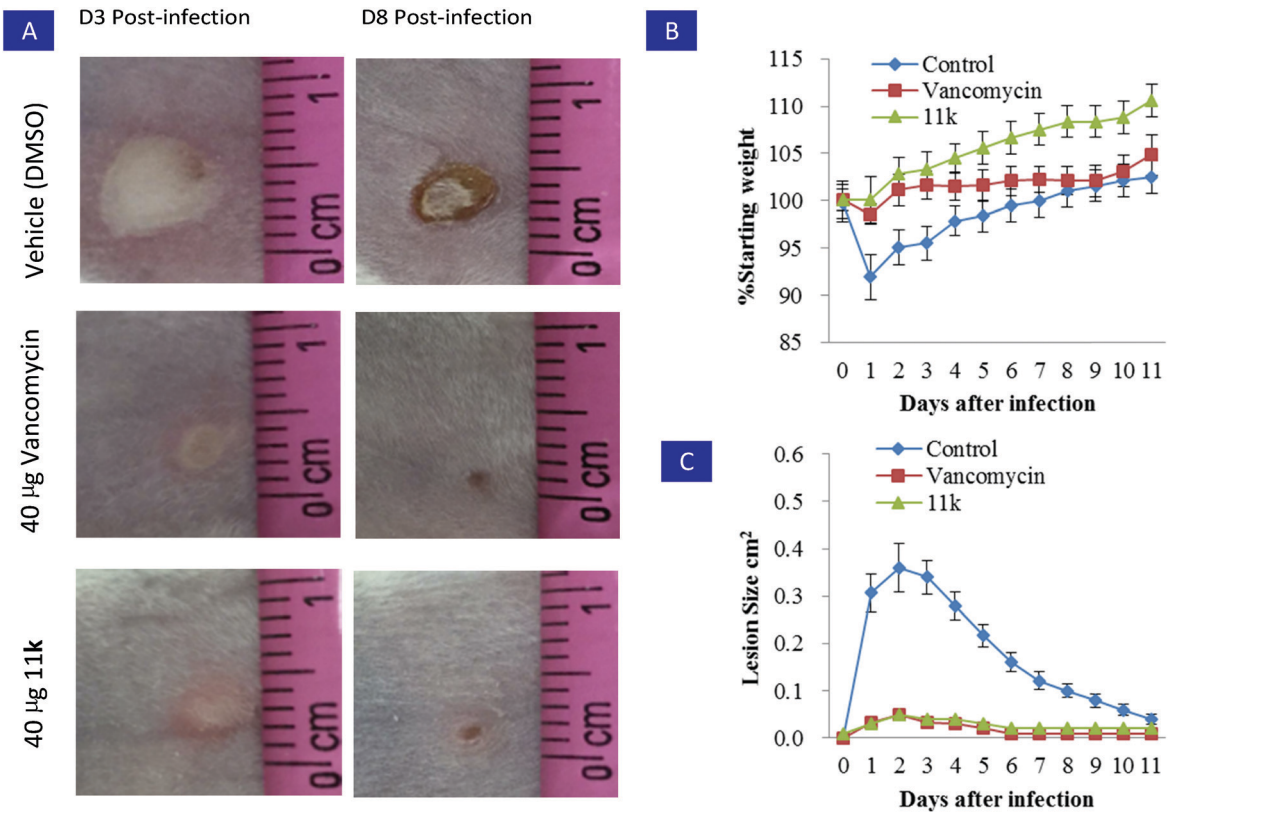

Fig. 5 Evaluation of RDSB analogue **11k** in a mouse model of skin infection. A) BALB/c mice were intradermally challenged with an inoculum mixture containing 1×10^8 CFU of MRSA (JCSC 4788) along with 40 μg of the vehicle control (DMSO) or 40 μg of **11k** or vancomycin. Representative images of the resulting cutaneous injuries sustained in the antibiotic and vehicle control mice are shown for 3 days and 8 days post-infection (scale in cm), respectively. B) A single 40 μg dose of **11k** or vancomycin profoundly attenuated dermatopathology following cutaneous MRSA (JCSC 4788) challenge. C) A single 40 μg dose of **11k** or vancomycin reduced morbidity as measured by animal weight. Error bars represent the standard deviation, $n = 6$.

column chromatography was purchased from Qing Dao Hai Yang Chemical Industry Co. of China. ^{1}H NMR and ^{13}C NMR spectra were recorded on a Brüker Advance 500 instrument (^{1}H: 500 MHz, ^{13}C: 125 MHz). Chemical shifts were reported in parts per million relative to $CDCl_3$ (^{1}H NMR; 7.27 ppm, ^{13}C NMR; 77.00 ppm). The following abbreviations were used to explain the multiplicities: s = singlet, d = doublet, t = triplet, q = quartet, m = multiplet, br = broad. Mass spectrometric data were obtained using an ABI-Q Star Elite high resolution mass spectrometer. Dichloroethane (DCE) was distilled from calcium hydride. Yields refer to chromatographically purified products unless otherwise stated.

4.2. Chemical synthesis

4.2.1. General procedure for the synthesis of compounds 5d–5k. Aluminum trichloride (4 g, 40 mmol) was slowly and carefully added to a solution of phloroglucinol **3** (1.26 g, 10 mmol) in $CH_2ClCH_2Cl/PhNO_2$ (1 : 1, 50 mL) at 0 °C. After stirring at this temperature for 10 min under nitrogen atmosphere, acid chloride **4** (12 mmol) was added. Then, the ice bath was removed, and the mixture was stirred at 80 °C for 3 h. The crude reaction mixture was cooled to room temperature and quenched with water (100 mL). The mixture was extracted with EtOAc (5 × 100 mL), washed with brine, and concentrated under vacuum. The crude product was purified by flash chromatography (silica gel, hexane : EtOAc = 2 : 1) to provide the relative products **5d–5k** with yields ranging from 60–80%. Their spectra data were referenced to the reported relative references.

4.2.2. General procedure for the synthesis of intermediate compounds 5l–5v. To a solution of phloroglucinol **4** (630 mg, 5.0 mmol) in acid chloride **5** (6.0 mmol), was added methanesulfonic acid (1.45 g, 15 mmol). After stirring at room temperature for 10 min under nitrogen atmosphere, the mixture was stirred at 60–80 °C for another 1 h. Then, the crude mixture was cooled to room temperature and quenched with water (20 mL). The mixture was extracted with EtOAc (5 × 25 mL), washed with brine, and concentrated under vacuum. The crude product was purified by flash chromatography (silica gel, hexane : EtOAc = 2 : 1) to provide compounds **5l–5v** with yields ranging from 25–80%. Their spectra data were referenced to the reported relative references.

4.2.3. Synthesis of 4-acyl-5-hydroxy-2,2,6,6-tetramethylcyclohex-4-ene-1,3-dione 6. Sodium methoxide (7.18 g, 133 mmol) was slowly dissolved in anhydrous methanol (60 mL) at 0 °C. To this clear solution, acylphloroglucinol **5c** (2.75 g, 16.5 mmol) was added carefully and the mixture was stirred for 10 min under nitrogen atmosphere. After that, methyl iodide (14.2 mL, 228 mmol) was slowly added. The ice bath was then removed, and the mixture was stirred at room temperature for 24 h. The crude mixture was quenched with 2 N HCl (60 mL) and extracted with $CHCl_3$ (5 × 60 mL), washed with brine, and concentrated under vacuum. The crude product was purified by flash chromatography (silica gel, hexane : EtOAc = 5 : 1) to provide **6** (3.17 g, 14.2 mmol, 86% yield) as a yellow rod-like crystal. ^{1}H NMR (500 MHz, $CDCl_3$): δ 1.33 (s, 6H), 1.42 (s, 6H), 2.57 (s, 3H); ^{13}C NMR (125 MHz, $CDCl_3$): δ 23.8, 24.3, 27.4, 52.0, 56.7, 109.4, 196.7, 199.1, 201.7, 210.0.

4.2.4. Synthesis of syncarpic acid 7. A flame-dried 50 mL flask was charged with 6 N HCl (30 mL) and **6** (3.17 g, 14.2 mmol), and the reaction mixture was stirred vigorously under reflux for 24 h. The mixture was cooled to room temperature and extracted with EtOAc (5 × 50 mL). The combined organic phases were washed with brine (30 mL), dried over Na_2SO_4, and filtered. Removal of the solvent by rotary evaporation and purification by flash column chromatography (silica gel, hexane : EtOAc = 1 : 1) afforded **7** (2.17 g, 11.4 mmol, 80% yield). ^{1}H NMR (500 MHz, $CDCl_3$): ketone: δ 1.31 (s, 12H), 3.61 (s, 2H); enol: δ 1.40 (s, 12H), 5.74 (br d, J = 2.3 Hz, 1H), 8.00 (br s, 1H); ^{13}C NMR (125 MHz, $CDCl_3$): ketone: δ 21.8, 50.2, 59.1, 204.3, 208.9; enol: δ 24.5, 51.2, 59.1, 101.7, 191.9, 204.3, 212.6.

4.2.5. Synthesis of 2,2,4,4-tetramethyl-6-(isopentylidene) cyclohexane-1,3,5-trione 9. Syncarpic acid **7** (182 mg, 1.0 mmol) was dissolved in CH_2Cl_2 (8 mL), and isovaleraldehyde **8** (172 mg, 2.0 mmol) and proline (12 mg, 0.1 mmol) were added. The resulting mixture was stirred for 30 min at room temperature, then purified by 3 cm long flash chromatography (silica gel, CH_2Cl_2) to afford the desired product **9** (250 mg, 100% yield) as a colorless oil. ^{1}H NMR (500 MHz, $CDCl_3$): δ 0.95 (d, J = 6.7 Hz, 6H), 1.30 (s, 6H), 1.31 (s, 6H), 1.89 (m, J = 6.7 Hz, 1H), 2.59 (dd, J = 3.0, 3.0 Hz, 2H), 7.51 (dd, J = 3.0 Hz, 1H); ^{13}C NMR (125 MHz, $CDCl_3$): δ 21.9, 22.3, 22.6, 28.7, 38.9, 57.9, 58.6, 133.1, 159.1, 196.4, 199.5, 208.8. 42.6.

4.2.6. General procedure for the synthesis of acylphloroglucinol analogues 10. Sodium hydride (80 mg, 2.0 mmol, 60% in mineral oil) was carefully added to a solution of acylphloroglucinol **5** (1.0 mmol) in THF (10 mL), and then the unsaturated triketone **9** (125 mg, 0.5 mmol) in THF (4 mL) was slowly added. The resulting mixture was stirred for 0.5 h at room temperature, and then quenched with 1 N HCl (5 mL) and extracted with EtOAc (3 × 10 mL), washed with brine, and concentrated under vacuum. The crude product was purified by flash chromatography (silica gel, hexane : EtOAc = 10 : 1 to 2 : 1) to provide derivatives of the general structure **10** with yields ranging from 30% to 80%.

4.2.7. General procedure for the synthesis of RDSB analogues 11. Acylphloroglucinol analogues **10** (0.5 mmol) were added to a solvent of 5 mL toluene and heated to reflux, and PTSA (0.05 mmol) was then added. The reaction mixture was further stirred at that temperature for about 1 h until all of the starting materials disappeared by TLC detection. After cooling to room temperature, the mixture was directly purified through a short flash chromatography (silica gel; hexane : EtOAc = 5 : 1) to afford the desired products **11a–11v** as slightly brown solids. The NMR spectra of products **11a–11v** can be seen in the ESI.†

4.3. Animals

Six-week-old female BALB/c mice from Guangdong Provincial Laboratory Animal Public Service Center were housed at 23 ±

1 °C with a 12 h light–dark cycle with free access to standard pellet chow and water and allowed to acclimatize to the laboratory environment for 7 days in propylene cages. The animal studies were conducted according to the guidelines established by the National Institutes of Health for the care and use of laboratory animals, and the recommendations of the Animal Care and Use policies at the South China Agricultural University (Guangzhou, China). Procedures concerning animal treatments were reviewed and approved by the Animal Use Ethics Committee of South China Agricultural University (No. SCAU2017-C003).

4.4. Bacteria strains and cells

S. aureus (ATCC 29213), *S. aureus* (ATCC 6538), *S. aureus* (CMCC 26003), *B. cereus* (ATCC 10876), *P. acnes* (ATCC 6919), *E. faecalis* (ATCC 29212), *S. epidermidis* (ATCC 12228), *B. polymyxa* (GIM 1.467), *B. polymyxa* (ATCC 842), *E. coli* (ATCC 8739), *S. typhi* (CMCC 44102), *S. dysenteriae* (CMCC 51252), and *C. albicans* (ATCC 10231) were obtained from Guangdong Institute of Microbiology (Guangzhou, China). Vancomycin-resistant *Enterococcus faecium* (VRE, No. 151458137) isolated from the abdominal cavity of patients was donated by the first affiliated hospital of Sun Yat-Sen University, Guangzhou, China. The SCCmec-carrying clinical isolates of MRSA (JCSC 4788, JCSC 2172, JCSC 3063, JCSC 4469, JCSC 4744, NCTC 10442, N 315,3 85/2082) were kindly provided by K. Hiramatsu and T. Ito from Juntendo University (Tokyo, Japan). RAW 264.7 cells were obtained from Kunming Institute of Zoology, Chinese Academy of Sciences (Kunming, China). MCF-7 and SF-268 cancer cells were obtained from the Cell Bank of the Chinese Academy of Sciences (Shanghai, China).

4.5. Activity evaluation

4.5.1. Minimal inhibitory concentration (MIC) assays. MIC determinations were performed by Microbroth dilution in Mueller–Hinton broth medium (MHB) according to CLSI[30] guidelines. Furthermore, *P. acnes* was cultured in the MGC Anaero Pack. Resazurin was added as a visible indicator according to the established method.[31]

4.5.2. The selectivity over cytotoxic activity study. The selectivity over cytotoxic activity study was performed using the MTT [3-(4,5-dimethylthiazol-2-yl)-2,5-diphenyl tetrazolium bromide] assay. **11k** was applied at various concentrations (ranging from 1.5625 to 100 μg mL^{-1}) and the control cells were treated with DMSO at the highest concentration used in the test wells (0.5%).

4.5.3. Time-killing assays. Time-kill assays were carried out based on the guidelines of CLSI.[30] The overnight culture of cells (MRSA JCSC 4788) was adjusted in a 0.85% NaCl buffer to obtain a bacterial suspension with 10^6 to 10^7 CFU mL^{-1}. The inoculums were treated with various concentrations (0.5×, 1×, 2×, and 4× MIC) of **11k** and vancomycin at 35 °C. Aliquots were removed at 0.5 h, 2 h, 4 h, 8 h, and 24 h to measure viable plate counts. Similar results were obtained by two independent time-kill tests.

4.6. Mode of antimicrobial action of 11l

4.6.1. Cytoplasmic membrane depolarization analysis. The membrane potential of MRSA (JCSC 4788) with **11k** was investigated using a modified method.[32] Briefly, exponential phase cultures of MRSA (JCSC 4788) were washed and adjusted to an optical density at 620 nm (OD_{620}) of 0.1 with a buffer solution (5 mM HEPES at pH 7). 0.4 μM 3,3′-dipropylthiacarbocyanine [DiSC3(5)] as well as 100 mM KCl were added to the cell suspensions and incubated for 20 min at 37 °C with agitation. The desired concentration of **11k** was added, and the change in fluorescence was monitored at an excitation wavelength of 660 nm and at an emission wavelength of 670 nm.

4.6.2. SYTOX Green assay. This assay was performed according to the reported method.[33] Briefly, exponential phase cultures of MRSA (JCSC 4788) were washed and adjusted to an optical density at 620 nm (OD_{620}) of 0.4 with a 0.85% NaCl buffer. The bacterial suspension was incubated with serial concentrations of RDSB for a desired time, and then treated with 3 μM of SYTOX Green for 20 min. The fluorescence reading was monitored at an excitation wavelength of 504 nm and at an emission wavelength of 523 nm. Melittin, a cell lytic factor, was used as a positive control.

4.6.3. Visualization of bacterial membrane permeability. The MRSA cell suspension (OD_{620} 0.4) was treated with the desired concentrations of **11k** and vancomycin for 3 h, and then incubated with 3 μM of SYTOX Green. Finally, the suspension was fixed on glass slides and then observed by a fluorescence microscope (ZEISS Model Axioplan 2IE) with an excitation wavelength of 485 nm.

4.6.4. Scanning electron microscopy. For observation using scanning electron microscopy, exponential-phase bacteria were treated with the compounds at 8× MIC for 4 h at 37 °C. Then, the cells were washed twice, suspended in PBS, and prefixed in 0.1 M phosphate buffer (pH 7.2) containing 2% glutaraldehyde and 2.5% paraformaldehyde overnight. After washing 6 times with 0.1 M phosphate buffer, the samples were post-fixed in 1% osmium tetroxide for 2 h. After washing another three times with 0.1 M phosphate buffer, the samples were dehydrated through a graded ethanol series and subjected to freeze-drying (JFD-310, JEOL, Japan). Afterwards, the samples were mounted on stubs and coated with gold in a sputter coater (JFC-1600, JEOL, Japan), and then examined and photographed under a scanning electron microscope (JSM-6360LV, JEOL, Japan).

4.7. Resistance study

Resistance was defined as an increase of 4-fold more than the initial MIC.[34] For resistance research by sequential passaging, MRSA (JCSC 4788) cells incubated in the exponential phase at 37 °C were passaged into fresh MHB containing **11k** at a sub-inhibitory concentration, and then re-passaged at 24 h intervals until at least 20 passages were completed. The MIC was determined as described above.

4.8. Mouse skin infected model

0.1 mL of MRSA (JCSC 4788) cells (1×10^8 CFU per mouse) and either **11k** (40 μg diluted in DMSO) or vancomycin (40 μg diluted in DMSO) were injected intradermally into the abdominal skin of matched BALB/c mice (female, 18–20 g per mouse). The negative control mice were infected with DMSO as a vehicle. The body weight and lesion size of each mouse were determined once per day for 11 days after infection.

4.9. Data analysis

All assays were carried out in at least triplicate, and all of the results were found to be reproducible. The cytotoxicity assay, DiSC3(5) assay, SYTOX Green assay, and *in vivo* antimicrobial activity results were expressed in terms of the mean ± standard deviation (SD).

Conflicts of interest

The authors declare no conflict of interest.

Acknowledgements

We thank the National Natural Science Foundation of China (NSFC) (No. 81773602, 31600271, 81502949), the Natural Science Foundation of Guangdong Province (2015A030310482, 2016A030313149, 2016A010105015), the Strategic Resources Service Network Program on Plant Genetic Resources Innovation of the Chinese Academy of Sciences (No. ZSZC-005), Pearl River Science and Technology New Star Fund of Guangzhou (201605120849569), and the Frontier Science Key Program of Chinese Academy of Sciences (No. QYZDB-SSW-SMC018) for financial support.

References

1 D. M. Brogan and E. Mossialos, *Global. Health*, 2016, **12**, 1–7.
2 R. M. Klevens, M. A. Morrison and J. Nadle, *et al.*, *JAMA*, 2007, **98**, 1763–1771.
3 G. Taubes, *Science*, 2008, **321**, 356–361.
4 Centers for Disease Control and Prevention, *Antibiotic Resistance Threats in the United States*, 2013.
5 H. F. Chambers, *N. Engl. J. Med.*, 2005, **352**, 1485–1487.
6 G. J. Moran, A. Krishnadasan and R. J. Gorwitz, *et al.*, *N. Engl. J. Med.*, 2006, **355**, 666–674.
7 B. W. Frazee, J. Lynn and E. D. Charlebois, *et al.*, *Ann. Emerg. Med.*, 2005, **45**, 311–320.
8 I. M. Gould, *Int. J. Antimicrob. Agents*, 2009, **34**, S2–S5.
9 L. L. Han, L. K. McDougal and R. J. Gorwitz, *et al.*, *J. Clin. Microbiol.*, 2007, **45**, 1350–1352.
10 R. Goldburg, S. Roach and D. Wallinga, *et al.*, *Science*, 2008, **321**, 1294.
11 D. Hardej, C. R. Ashby Jr and N. S. Khadtare, *et al.*, *Eur. J. Med. Chem.*, 2010, **45**, 5827–5832.
12 F. R. DeLeo, M. Otto and B. N. Kreiswirth, *et al.*, *Lancet*, 2010, **375**, 1557–1568.
13 A. Anandan, G. L. Evans and M. L. O'Mara, *et al.*, *Proc. Natl. Acad. Sci. U. S. A.*, 2017, **114**, 2218–2223.
14 H. X. Liu, W. M. Zhang and Z. F. Xu, *et al.*, *RSC Adv.*, 2016, **6**, 25882–25886.
15 H. X. Liu, H. B. Tan and S. X. Qiu, *et al.*, *J. Asian Nat. Prod. Res.*, 2016, **18**, 535–541.
16 J. J. Koh, S. M. Lin and T. T. Aung, *et al.*, *J. Med. Chem.*, 2015, **58**, 739–752.
17 H. B. Tan, H. X. Liu and L. Y. Zhao, *et al.*, *Eur. J. Med. Chem.*, 2017, **125**, 492–499.
18 S. Dachriyanus, M. V. Sargent and B. W. Skelton, *et al.*, *Aust. J. Chem.*, 2002, **55**, 229–232.
19 S. Leejae, L. Hasap and S. P. Voravuthikunchai, *J. Med. Microbiol.*, 2013, **62**, 421–428.
20 S. Leejae, P. W. Taylor and S. P. Voravuthikunchai, *J. Med. Microbiol.*, 2013, **62**, 78–85.
21 M. Morkunas, L. Dube, F. Götz and M. E. Maier, *Tetrahedron*, 2013, **69**, 8559–8563.
22 H. X. Liu, K. Chen and Y. Yuan, *et al.*, *Org. Biomol. Chem.*, 2016, **14**, 7354–7360.
23 I. R. Green, F. E. Tocoli and S. H. Lee, *et al.*, *Med. Chem.*, 2007, **15**, 6236–6241.
24 The biophysical processes mainly referred to that the hydrophilic head moiety binds with an intermolecular hydrogen bond like a 'hook' attaching itself to a hydrophilic portion of the membrane, after which the hydrophobic tail portion of the molecule is then able to enter into the membrane lipid bilayer (ref. 23).
25 R. M. Epand, S. Rotem and A. Mor, *et al.*, *J. Am. Chem. Soc.*, 2008, **130**, 14346–14352.
26 S. R. Singh, A. E. Bacon and D. C. Young, *et al.*, *Antimicrob. Agents Chemother.*, 2009, **53**, 4495–4497.
27 P. Vergidis, M. S. Rouse and G. Euba, *et al.*, *Antimicrob. Agents Chemother.*, 2011, **55**, 1182–1186.
28 I. H. Eissa, H. Mohammad and O. A. Qassem, *et al.*, *Eur. J. Med. Chem.*, 2017, **130**, 73–85.
29 J. J. Koh, S. X. Qiu and H. X. Zou, *et al.*, *Biochim. Biophys. Acta*, 2013, **1828**, 834–844.
30 CLSI, *Performance standards for antimicrobial susceptibility testing, twenty-first informational supplement CLSI document*, 2011, M100–S21.
31 A. J. Drummond, *Recent Res. Dev. Phytochem.*, 2000, **4**, 143–152.
32 M. Wu, E. Maier and R. Benz, *et al.*, *Biochemistry*, 1999, **38**, 7235–7242.
33 R. Rathinakumar, W. F. Walkenhorst and W. C. Wimley, *J. Am. Chem. Soc.*, 2009, **131**, 7609–7617.
34 D. J. Farrell, M. Robbins and W. Rhys-Williams, *et al.*, *Antimicrob. Agents Chemother.*, 2011, **55**, 1177–1181.